Flood risk assessment at the regional scale: Computational challenges and the monster of uncertainty (1)

EGU General Assembly 2016, Vienna, Austria, 17-22 April 2016

Session HS7.5/NH1.21: *Hydroclimatic extremes under change: advancing the science and implementation in hazard prevention and control*

A. Efstratiadis[(1)], S.-M. Papalexiou[(1)], Y. Markonis[(1)], A. Koukouvinos[(1)], L. Vasiliades[(2)], G. Papaioannou[(2)], and A. Loukas[(2)]

(1) Department of Water Resources and Environmental Engineering, National Technical University of Athens, Greece

(2) Department of Civil Engineering, University of Thessaly, Volos, Greece

1. Abstract

We present a methodological framework for **flood risk assessment at the regional scale**, developed within the implementation of the EU Directive 2007/60 in Greece. This comprises three phases: (a) **statistical analysis of extreme rainfall data**, resulting to spatially-distributed parameters of intensity-duration-frequency (IDF) relationships and their confidence intervals, (b) **hydrological simulations**, using event-based semi-distributed rainfall-runoff approaches, and (c) **hydraulic simulations**, employing the propagation of flood hydrographs across the river network and the mapping of inundated areas. The flood risk assessment procedure is employed over the River Basin District of Thessaly, Greece, which requires schematization and modelling of hundreds of sub-catchments, each one examined for several risk scenarios. This is a challenging task, involving multiple computational issues to handle, such as the organization, control and processing of huge amount of hydro-meteorological and geographical data, the configuration of model inputs and outputs, and the co-operation of several software tools. In this context, we have developed supporting applications allowing **massive data processing** and **effective model coupling**, thus drastically reducing the need for manual interventions and, consequently, the time of the study. Within flood risk computations we also account for three major sources of uncertainty, in an attempt to provide **upper and lower confidence bounds of flood maps**, i.e. (a) statistical uncertainty of IDF curves, (b) structural uncertainty of hydrological models, due to varying antecedent soil moisture conditions, and (c) parameter uncertainty of hydraulic models, with emphasis to roughness coefficients. Our investigations indicate that the combined effect of the above uncertainties (which are certainly not the unique ones) result to **extremely large bounds of potential inundation**, thus rising many questions about the interpretation and usefulness of current flood risk assessment practices.

2. Problem statement, study area and assumptions

- **Key objective of the study**: Establishing flood hazard and flood risk maps to assess the potential adverse consequences to human health, the environment, cultural heritage and economic activities, for three characteristic return periods (T = 50, 100, 1000 years).
- **Study area**: Water District of Thessaly, Greece, with emphasis to flood prone zones, spanning over 4 200 out of 13 500 km^2 of the total area (Fig. 1).
- **Modelling framework**: Event-based deterministic approach, comprising three modelling components: (a) synthetic storm generator; (b) hydrological simulation model; and (c) hydraulic simulation model.
- **Key assumption**: Flood risk is determined in terms of return period of input rainfall.
- **Representation of uncertainties**: Scenario-based approach, considering specific sources of uncertainty associated with the three modelling components.
- **Final outcome**: Flood risk maps (three for each return period), corresponding to the "average" hydrological scenario and its uncertainty bounds (upper, lower).

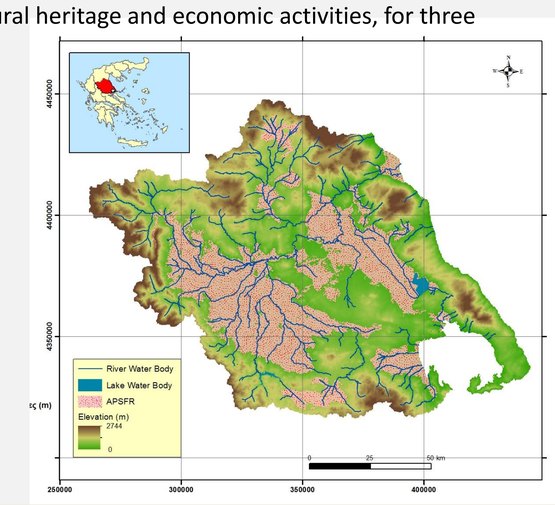

***Fig. 1**: Study area and flood prone zones, as determined in the context of the preliminary flood risk assessment (EU Directive 2007/60, Article 4).*

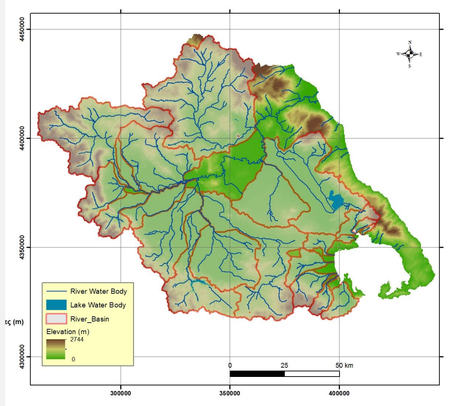

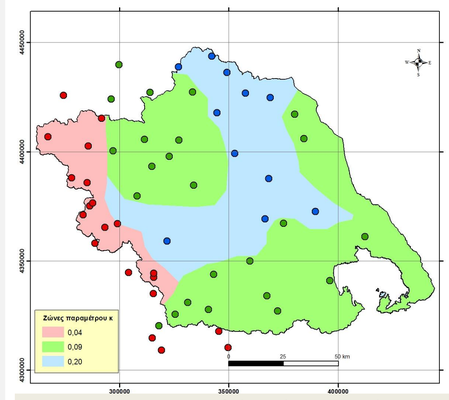

***Fig. 2**: Discretization of Thessaly into river basins (upper map), and formulation of climatic zones according to shape parameter k (lower map).*

3. Overview of flood modelling approach

- The study area has been divided into 22 **river basins** (Fig. 2, up), each one represented through conceptual semi-distributed modelling schemes, comprising **sub-basins**, **reaches** and **junctions**.
- Two levels of analysis were employed:
  - **Hydrological analysis** across river basins (divided into 351 sub-basins, in total), using the HEC-HMS software;
  - **Hydraulic analysis** along selected reaches, specifically those crossing flood prone zones (also termed Areas of Potential Flood Risk, APFR), using alternative numerical schemes and associated modelling tools.
- Input of the hydrological simulation of each sub-basin was the **synthetic hyetograph** of each return period of interest (using the alternative blocks method, for T = 50 and 100 years, and the worst profile method, for T = 1000 years), while input for the hydraulic simulation of each reach of interest was the **simulated hydrograph** of the corresponding upstream junction.
- The method uses as overall input **intensity-duration-frequency (IDF) relationships**, referred to the sub-basin scale, which have been estimated through statistical analysis of the observed **extreme rainfall data** across the broader study area.
- Extreme rainfall records of at least 15 years length over years 1950-2012 were collected from **71 stations**, well-distributed over Thessaly (Fig. 2, down), which comprise two types of data:
  - Annual series of maximum intensities at 15 recording stations (pluviographs), most of which of 0.5 h time resolution, that were available for durations 0.5, 1, 2, 6, 12, 24 and 48 h;
  - Annual series of maximum daily and two-day rainfall depths for the above 15 stations as well as 55 non-recording rain gauges.
- Raw data has been subject to several **empirical, graphical and statistical tests** and associated processing, in order to locate and remove erroneous or suspicious values associated with random as well as systematic errors.
- At each station we assigned an IDF expression proposed by Koutsoyiannis *et al*. (1998), representing the average rainfall intensity i over a timescale (also referred to as duration) d, for a given return period T as the ratio of a Generalized Pareto distribution for rainfall intensity over some threshold at any timescale (Koutsoyiannis, 2004) to a duration function, i.e.:

$$i(d, T) = \lambda' \, (T^{\kappa} - \psi') \, / \, (1 + d/\vartheta)^{\eta}$$

  where λ', ψ', κ, ϑ and η are parameters that were estimated using a stepwise approach, which is briefly described in section 4.
- The IDFs have been **parameterized** over Thessaly (Fig. 2, down, and Fig. 3), thus allowing the determination of **spatially-distributed hyetographs** (different rainfall inputs were assigned to each sub-basin).

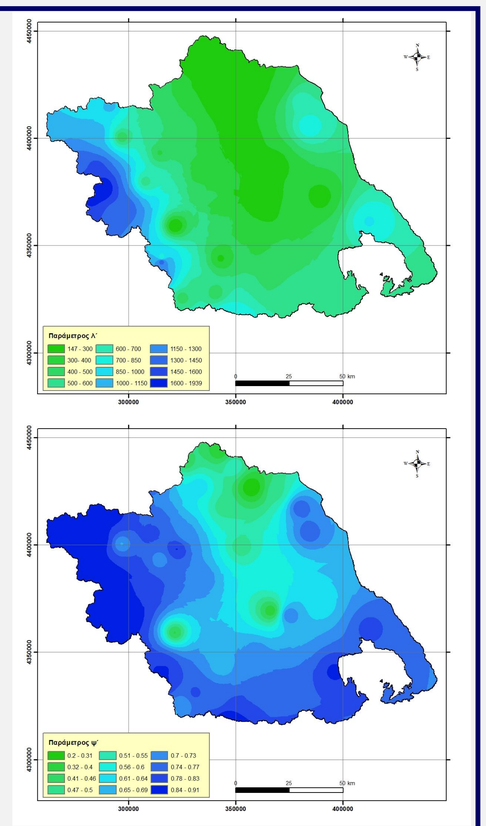

***Fig. 3**: Interpolation maps of spatially distributed scale and location parameters λ' (up) and ψ' (down).*

4. IDF parameters and confidence intervals estimation

- Parameters ϑ and η of **the duration function** were estimated by minimizing the Kruskal-Wallis statistic against the compound (unified) sample of finely-resolved data from the 15 recording stations. The optimal values were ϑ = 0.042 h and η = 0.639, which are considered constant over the study area.
- At each of the 71 stations, the parameter κ (which is actually the shape parameter of a GEV-max distribution) has been initially estimated on the basis of maximum 24 h data, by employing the technique by Papalexiou and Koutsoyiannis (2013), in order to adjust the **biased estimations** provided by the standard L-moments approach, thus accounting for the statistical uncertainty induced due to **small samples**. This approach prohibits obtaining too large shape parameter values, which are due to outliers, or negative κ values, which are statistically inconsistent (Fig. 4).
- Based on their **shape parameter** value, all stations were grouped into **three climatic zones** (Fig. 2, down), where we assigned common values, i.e. κ_1 = 0.04 (western zone located in the leeward part of Pindus), κ_2 = 0.09 (NW and SE areas), and κ_3 = 0.20 (plain areas and areas located in the windward part of Olympus).
- Point values of **scale and location parameters** λ' and ψ', respectively, were estimated by employing the L-moments method to the compound sample of each station assigned to a specific climatic zone, considering the given values of ϑ, η and κ.
- We generated empirical 80% **confidence intervals** of point rainfall estimations for T = 50, 100 and 1000 years, by employing **Monte Carlo simulations against scale and location parameters** λ' and ψ' (wider ranges are obtained as the return period increases).

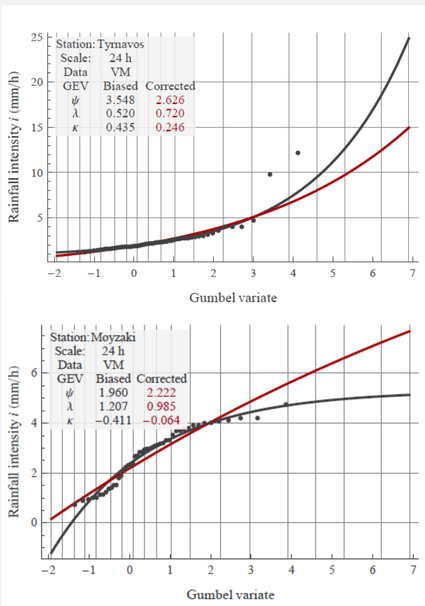

***Fig. 4**: Fitting of GEV distribution to daily rainfall maxima of two stations, considering biased and unbiased estimations of shape parameter κ.*

5. Hydrological model assumptions and representation of uncertainties

- We used the **SCS-CN method** to estimate the effective rainfall at the sub-basin scale, considering three hydrological scenarios per return period.
- Scenarios were determined by combining three (i.e., dry, average, wet) **antecedent soil moisture conditions (AMC)**, resulting to different CN values, with rainfall intensities provided by the IDF relationship and its 80% confidence limits, which are measure of **rainfall uncertainty**.
- The 20% lower rainfall estimation limit was assigned to CN1 and the 80% upper to CN3, thus representing the **joint uncertainty** associated with rainfall parameters λ' and ψ', and the key hydrological parameter, CN, which is actually a random variable (Efstratiadis *et al.*, 2014).
- Inflows to the river network are the hydrographs generated across the river basin, which are estimated by propagating the effective rainfall by each sub-basin to its outlet junction, via the **unit hydrograph** theory.
- We applied the **dimensionless synthetic unit hydrograph** (SUH) by SCS, that uses as sole input the time of concentration, t_c, of each sub-basin.
- In order to account for the **dependence of flow velocity to discharge**, t_c was considered decreasing function of rainfall, using the empirical rule:

$$t_c(T) = t_c \sqrt{i(5) \,/\, i(T)}$$

  where t_c is estimated by the Giandotti formula, assumed representative for flood events up to T = 5 years, $i(5)$ is the 5-year rainfall intensity, and $i(T)$ is the intensity corresponding to the return period of interest.
- The changing t_c introduces further nonlinearity to rainfall-runoff processes, and provides **more disadvantageous SUHs**, which become more narrow as the rainfall associated with T and its uncertainty bounds increases (Fig. 5).

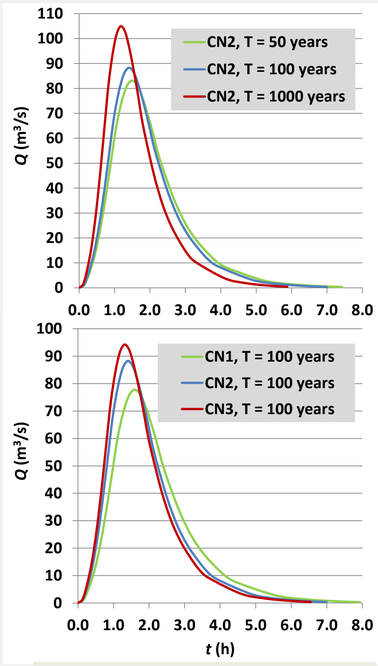

***Fig. 5**: Adjustment of unit hydrograph for different return periods (up) and different CN values, associated with average and 80% confidence limits of rainfall (down).*

Flood risk assessment at the regional scale: Computational challenges and the monster of uncertainty (2)

EGU General Assembly 2016, Vienna, Austria, 17-22 April 2016

Session HS7.5/NH1.21: *Hydroclimatic extremes under change: advancing the science and implementation in hazard prevention and control*

A. Efstratiadis[(1)], S.-M. Papalexiou[(1)], Y. Markonis[(1)], A. Koukouvinos[(1)], L. Vasiliades[(2)], G. Papaioannou[(2)], and A. Loukas[(2)]

(1) Department of Water Resources and Environmental Engineering, National Technical University of Athens, Greece

(2) Department of Civil Engineering, University of Thessaly, Volos, Greece

6. Semi-distributed hydrological simulation of Xerias river basin

- The methodology is demonstrated to the case of Xerias river basin of (116.8 km^2), which originates from Pelion and drains the southern part of the City of Volos, often causing severe floods (Fig. 6).
- Within the semi-distributed configuration employed in the HEC-HMS environment (Fig. 7), the basin is divided into **10 sub-basins** that exhibit significant heterogeneity, since their CN2 values (corresponding to AMC-II conditions) range from 50 to 82, while their 24-h rainfall depths for T = 100 years range from 198 to 253 mm.
- The river network is represented by means of **7 junctions** and **6 reaches**, with average slopes ranging from 5.0% (upper course) to 0.3% (lower course).
- In order to provide realistic estimations of the **timing of hydrograph arrivals** across the river network, which are inputs to the hydraulic simulation model, we employed simplified hydrological routing approaches, particularly the lag routing method, for relatively steep slopes (>1%), and the Muskingum method, for milder slopes.
- The **travel time** along each reach j, which is parameter of both routing methods, was computed as the ratio of the channel length L_j to a characteristic velocity u_j, given by:

$$u_j = k\, s_j^{1/2}$$

  where s_j is the average slope of the reach and k is a global parameter of the river basin.
- For each return period and each AMC scenario, parameter k was adjusted such as the travel time across the longest flow path (i.e., from the most upstream sub-basin to the outlet junction) equals the **varying time of concentration** of the river basin; the latter ranges from 5.1 h for T =5 years (reference value, provided via the Giandotti formula) to 2.6 h, which corresponds to the upper 80% confidence limit of the 24-h rainfall over the basin for T = 1000 years (Fig. 8).
- Synoptic results at the basin scale for the 3×3 = 9 scenarios, highlighting the astonishing **uncertainty** associated with rainfall-runoff modelling, are given in the following table.

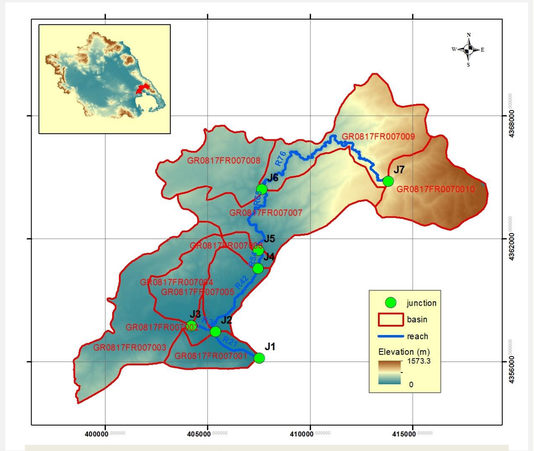

***Fig. 6**: Elevation map of Xerias river basin and geographical data (sub-basins, junctions, reaches).*

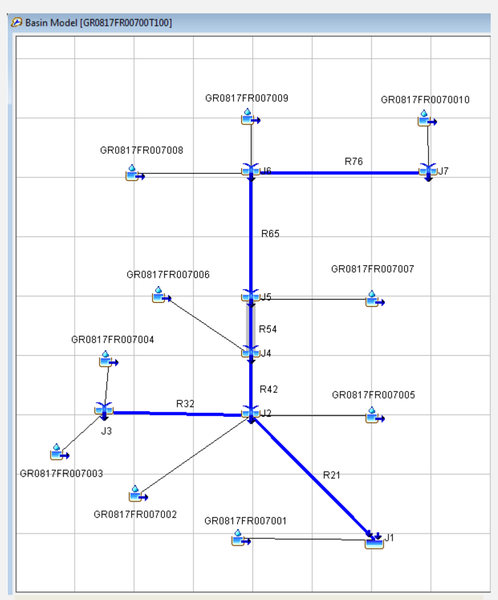

***Fig. 7**: Schematic representation of modeling components of Xerias river basin in the HEC-HMS environment.*

Return period (years)	Lower rainfall scenario & dry AMC (CN1)	Normal rainfall scenario & average AMC (CN2)	Upper rainfall scenario & wet AMC (CN3)
	Total rainfall depth (mm)		
T = 50	162.6	189.3	213.1
T = 100	177.9	215.5	251.7
T = 1000	222.9	315.2	431.3
	Total flood depth (mm)		
T = 50	20.7	79.7	146.9
T = 100	26.3	99.4	182.9
T = 1000	45.9	181.0	355.8
	Runoff coefficient of flood event		
T = 50	0.127	0.421	0.689
T = 100	0.148	0.461	0.727
T = 1000	0.206	0.574	0.825
	Peak discharge (m^3/s)		
T = 50	81.8	414.2	820.4
T = 100	108.4	543.1	1063.6
T = 1000	357.4	1265.9	2287.9
	Flood runoff volume (hm^3)		
T = 50	3.859	10.744	18.602
T = 100	4.663	13.199	22.958
T = 1000	7.479	23.270	43.681

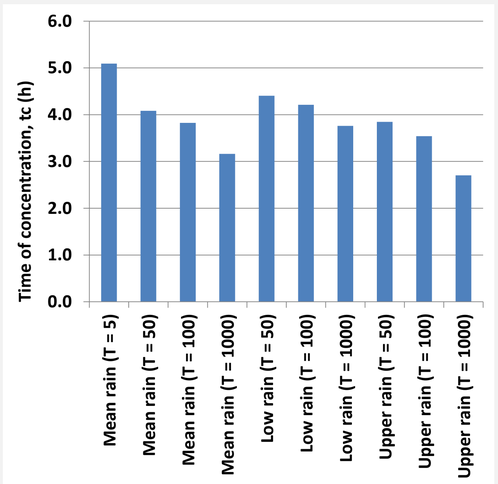

***Fig. 8**: Change of the time of concentration of Xerias basin against different return periods and hydrological scenarios, expressed in terms of 24-h rainfall intensity.*

7. Hydraulic simulation of lower course of Xerias river basin

- The model domain extends downstream of junction J4 and involves three reaches (R42, R32, R21), crossing **urban areas** of Volos.
- **Historical flood inundation data** was used for validation of the methodology and evaluation of alternative models, configurations and assumptions (Papaioannou *et al.*, 2015, 2016).
- We used the **HEC-RAS 2D** model with:
  - flexible mesh size (average 14 m);
  - 2D diffusion wave solution;
  - computation interval 2.0 s.
- The input DEM was created by employing **aerial imagery techniques** with 5 m cell size, while buildings over urban areas were represented via the **elevation rise method**.

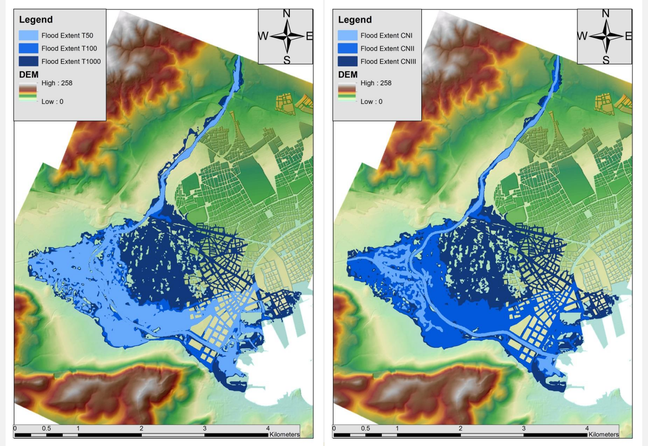

***Fig. 9**: Flood extent for all return periods of interest (T = 50, 100 & 1000 years), by employing the "average" hydrological scenario with "average" roughness coefficients (left), and overall uncertainty bounds of flood extent for T = 100 years, considering the most favorable and unfavorable combinations of input rainfall, antecedent soil moisture conditions and roughness coefficients (right).*

- **Flood mitigation works** have been merged with DEM, and the rest technical infrastructures (bridges, etc.) have been processed through specific modules that are available in the HEC-RAS platform.
- Inputs of hydraulic modeling were hydrographs provided by "average" hydrological simulation scenarios, by assigning "average" **roughness coefficients** that were estimated according to CORINE 2000 land use classes.
- For all return periods, apart from the hydrographs provided by the lower and upper scenarios, we also perturbed the roughness values by -50% and +50%, respectively, to obtain **overall uncertainty bounds of inundated areas** (Fig. 9) and associated hydraulic quantities, i.e. **water depths** and **velocities** (Fig. 10).

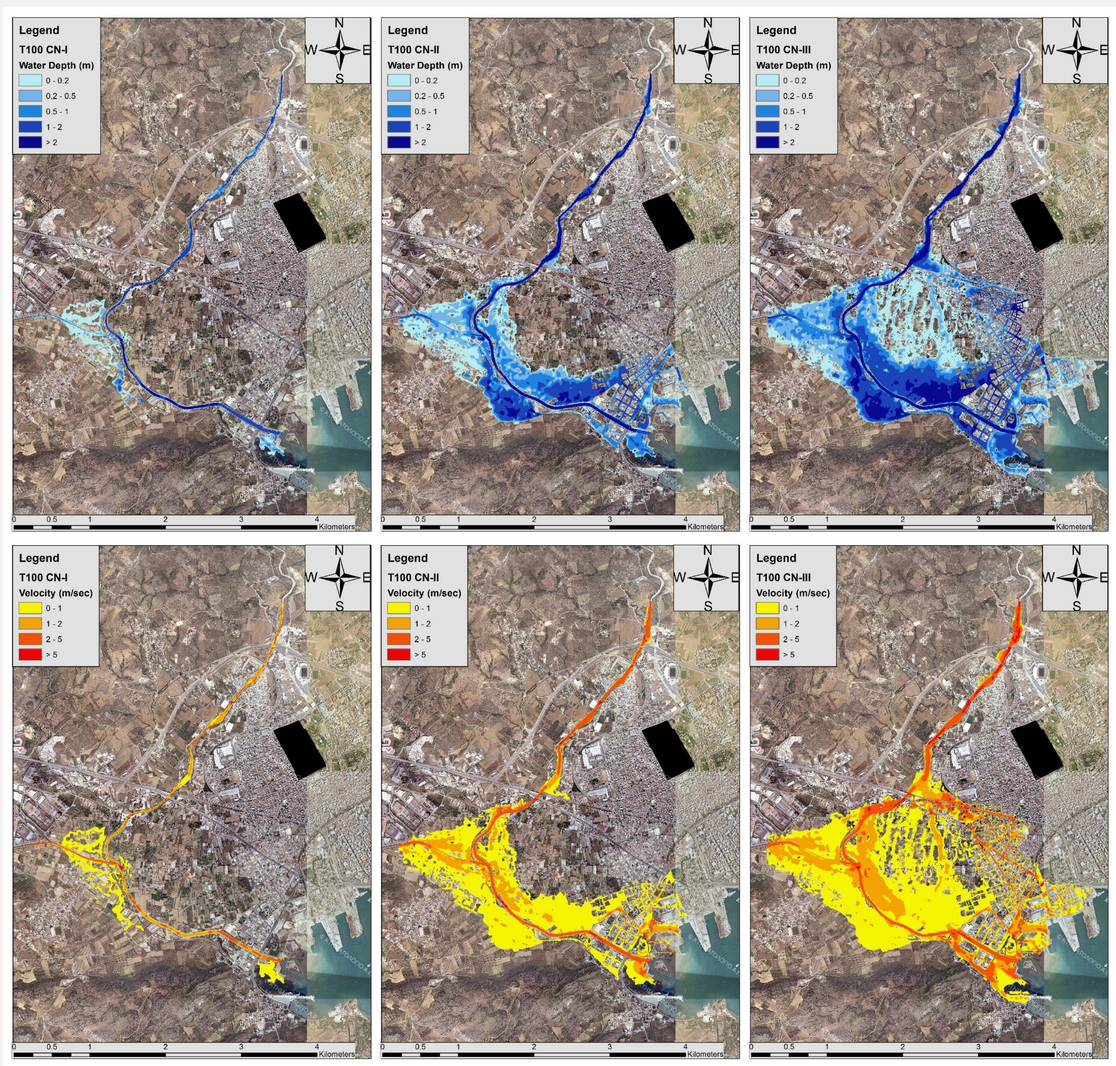

***Fig. 10**: Simulated water depths (up) and velocities (down) considering the combined scenarios for T = 100 years; in the middle maps are shown the average scenarios, in the left maps the lower bound scenarios, and in the right maps the upper bound scenarios.*

8. Flood engineers vs. uncertainty: is it possible to beat the monster?

- In the context of flood simulations, we attempted quantifying three major sources of uncertainty:
  - **Statistical uncertainty** associated with two (out of five) parameters of IDF relationships (i.e., scale and location parameters), originating from small samples of observed extreme rainfall data;
  - Uncertainty associated with **initial soil moisture conditions** of the hydrological model, resulting to a wide range of the key input parameter of the SCS-CN method, i.e. the potential maximum retention;
  - **Parametric uncertainty** associated with the Manning's roughness coefficient, which is typical input of hydraulic and hydrodynamic simulation models.
- Results are rather disappointing, since the uncertainty bounds of all major flood quantities (peak flows, flood volumes, inundated areas, etc.) **strongly overlap** the risk expressed in terms of return period of rainfall, while for large return periods, the lower and upper estimations may differ **one order of magnitude**.
- There are **numerous additional sources of uncertainty** that have been ignored in this study, involving the rest three IDF parameters (particularly the shape parameter κ, which is very sensitive), the spatiotemporal distribution of the design rainfall, hydrological parameters such as the time of concentration, the initial abstraction, the time to peak and base time of the SUH, as well as several assumptions associated with the geometrical properties and the numerical scheme of hydraulic simulation (cf. Dimitriadis *et al.*, 2016).
- In order to beat the monster, a key step is recognizing that **uncertainty is intrinsic**, and the unique means to reduce it is the use of **data**, which may ensure better estimations of model parameters through **calibration**.

9. References

- Dimitriadis, P., A. Tegos, A. Oikonomou, V. Pagana, A. Koukouvinos, N. Mamassis, D. Koutsoyiannis, and A. Efstratiadis, Comparative evaluation of 1D and quasi-2D hydraulic models based on benchmark and real-world applications for uncertainty assessment in flood mapping, *Journal of Hydrology*, 534, 478–492, doi:10.1016/j.jhydrol.2016.01.020, 2016.
- Efstratiadis, A., A. D. Koussis, D. Koutsoyiannis, and N. Mamassis, Flood design recipes vs. reality: can predictions for ungauged basins be trusted?, *Natural Hazards and Earth System Sciences*, 14, 1417–1428, doi:10.5194/nhess-14-1417-2014, 2014.
- Koutsoyiannis, D., D. Kozonis, and A. Manetas, A mathematical framework for studying rainfall intensity-duration-frequency relationships, *Journal of Hydrology*, 206 (1-2), 118–135, 1998.
- Koutsoyiannis, D., Statistics of extremes and estimation of extreme rainfall, 1, Theoretical investigation, *Hydrological Sciences Journal*, 49(4), 575–590, 2004.
- Papaioannou, G., A. Loukas, L. Vasiliades, and G. T. Aronica, Flood inundation mapping sensitivity to riverine spatial resolution and modelling approach, *Natural Hazards*, 2016 (submitted).
- Papaioannou, G., L. Vasiliades, and A. Loukas, Multi-criteria analysis framework for potential flood prone areas mapping, *Water Resources Management*, 29, 399-418, doi:10.1007/s11269-014-0817-6, 2015.
- Papalexiou, S.M., and D. Koutsoyiannis, Battle of extreme value distributions: A global survey on extreme daily rainfall, *Water Resources Research*, 49(1), 187–201, doi:10.1029/2012WR012557, 2013.